ADVANCED MATERIALS
www.advmat.de

Thread-Like Radical-Polymerization via Autonomously Propelled (TRAP) Bots

Sarvesh Kumar Srivastava, Fatemeh Ajalloueian, and Anja Boisen*

Micromotor-mediated synthesis of thread-like hydrogel microstructures in an aqueous environment is presented. The study utilizes a catalytic micromotor assembly (owing to the presence of a Pt layer), with an on-board chemical reservoir (i.e., polymerization mixture), toward thread-like radical-polymerization via autonomously propelled bots (i.e., TRAP bots). Synergistic coupling of catalytically active Pt layer, together with radical initiators (H_2O_2 and $FeCl_3$ (III)), and PEGDA monomers preloaded into the TRAP bot, results in the polymerization of monomeric units into elongated thread-like hydrogel polymers coupled with self-propulsion. Interestingly, polymer generation via TRAP bots can also be triggered in the absence of hydrogen peroxide for cellular/biomedical application. The resulting polymeric hydrogel microstructures are able to entrap living cells (NIH 3T3 fibroblast cells), and are easily separable via a centrifugation or magnetic separation (owing to the presence of a Ni layer). The cellular biocompatibility of TRAP bots is established via a LIVE/DEAD assay and MTS cell proliferation assay (7 days observation). This is the first study demonstrating real-time in situ hydrogel polymerization via an artificial microswimmer, capable of enmeshing biotic/abiotic microobjects in its reaction environment, and lays a strong foundation for advanced applications in cell/tissue engineering, drug delivery, and cleaner technologies.

Self-propelled artificial microswimmers (or micromotors) have made a significant contribution in the field of drug delivery,[1] stimuli-responsive systems,[2] and bioinspired microrobotics.[3] This has been possible not only because of their autonomous propulsion, but more so because of their ability to ferry a specific payload (like drug),[4] or capture a specific target (like value added product).[5,6] These artificial microswimmers utilizes a catalytically active layer and/or solid fuel, which reacts with the aqueous microenvironment, thereby initiating a gas evolution reaction for autonomous propulsion (among others).[7,8] Recent research exploring surface-based effects on self-propulsion and associated transport characteristics has pushed the research in the area of artificial microswimmer toward remote transporting of matter at microscale.[9–11] In general, trapping of objects via a self-propelled swimmer at microscale is a challenge due to the strongly reduced size of the traps and altered asymmetry for propulsion. To this end, Löwen and coworkers reported a theoretical model in which static chevron-shaped structures can be used to trap self-propelled rod-like particles.[12,13] Additionally, ratchets of different geometries have been reported to redirect the motion of motile entities such as bacteria and molecular motors.[14,15] Likewise, Wilson et al. demonstrated entrapment of Pt nanoparticles (NPs) with polymerosomes (coblock polymer), such that the incorporated NPs decompose H_2O_2 for autonomous propulsion (O_2) evolution.[16]

However, all reported studies focus on a prefabricated polymeric or metallic micromotor assembly—there exist no study till date reporting an artificial microswimmer, with an on-board in situ polymerization system, capable of real time deployment of a "hydrogel mesh" for target capturing. To this end, nanoporous hydrogels are of significant interest owing to their practical relevance in the area of cell/tissue culturing,[17] molecular filtration/separation,[18] controlled drug release,[19] and as sensors and actuators.[20,21] A report by Orive et al.[22] highlighted the importance of cell trapping/enmeshing as: a) therapeutic cell encapsulation for dynamic release of active compounds in response to external stimuli, b) real-time cell trapping and differentiation via remote assembly for regenerative medicine applications, and c) 3D-culture system for mass production in bioreactors.

Here, we report in situ polymerization of acrylate monomers into elongated thread-like polymeric structures, which can remotely entrap living cells as well as abiotic microobjects (polystyrene microparticles). We chose acrylate-based hydrogel system owing to its biocompatible nature, where rapid hydrogel formation proceeds via a radical polymerization mechanism as shown in **Figure 1**A.[23,24] Clearly, incorporating a heterogeneous catalyst like Pt will drastically increase the peroxide decomposition, thereby, generating more free radicals in the process (for rapid polymerizations) coupled with bubble propulsion. In the absence of hydrogen peroxide, polymerization will still proceed, albeit without bubble propulsion (O_2 evolution). We utilized a Su-8 photopolymer based cylindrical

Dr. S. K. Srivastava, Dr. F. Ajalloueian, Prof. A. Boisen
Center for Intelligent Drug Delivery and Sensing Using Microcontainers and Nanomechanics (IDUN)
Department of Healthcare Technology
Technical University of Denmark
2800 Lyngby, Denmark
E-mail: sarvesh.kumar@dtu.dk

The ORCID identification number(s) for the author(s) of this article can be found under https://doi.org/10.1002/adma.201901573.

DOI: 10.1002/adma.201901573

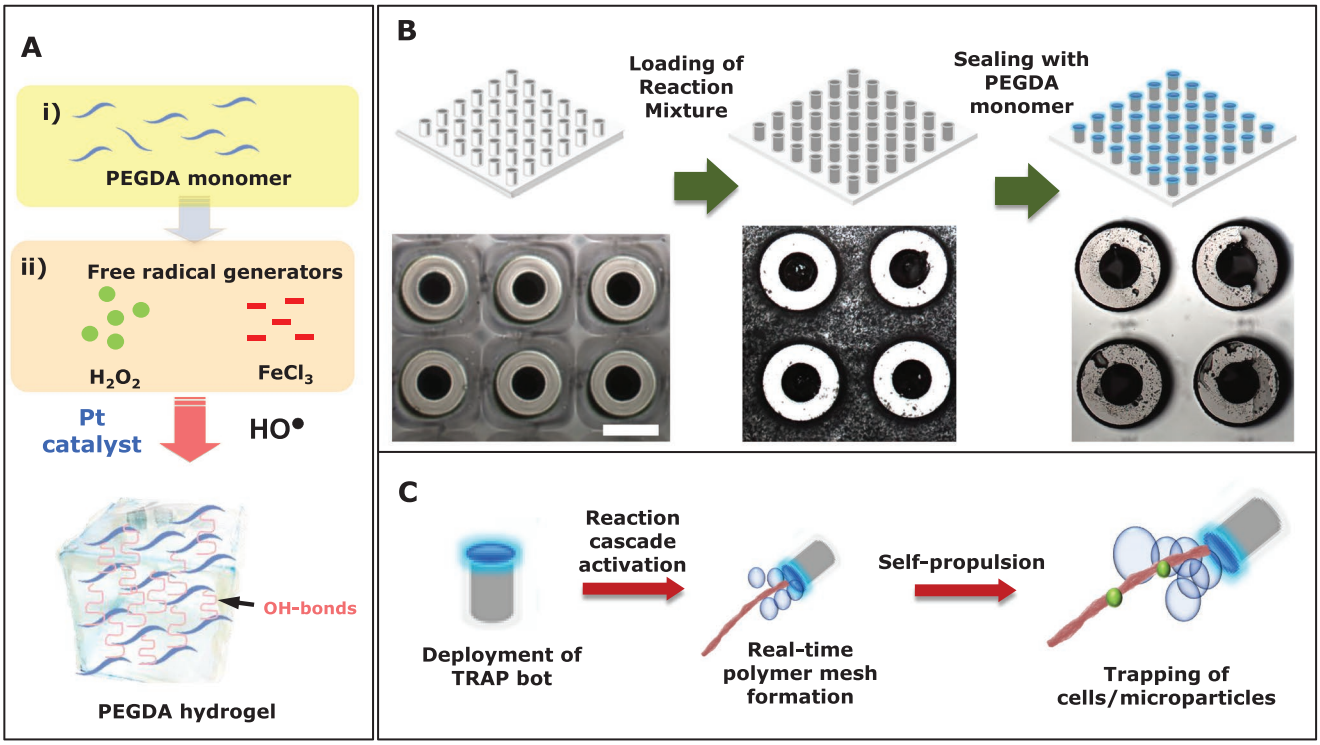

Figure 1. A–C) Schematic representation of PEGDA polymerization (A), TRAP bot fabrication (B), and TRAP bot activation (C). Scale bar: 250 µm.

design with one end enclosed, thereby, providing a distinct internal cavity coated with a thin layer of Ni/Pt metal (10 nm). Resulting TRAP bots were of dimension: height 220 µm and inner diameter 190 µm with a sealed bottom, as depicted in Figure 1B. Refer to Supporting Information for TRAP bot chassis fabrication. Upon TRAP bot chassis fabrication, the grid incorporating the bots was coated with a thin layer of poly(dimethylsiloxane) (PDMS) overlay (without covering them on top) acting as a negative shadow mask. This ensured uniform loading of reaction mixture into the TRAP bot's reaction chamber only. Finally, a reaction mixture comprising of ascorbic acid (i.e., Vitamin C) and $FeCl_3$ (III) was loaded, and resulting microassembly was sealed-off with a layer of poly(ethylene glycol) diacrylate (PEGDA) monomer. TRAP bots when deployed in its aqueous reaction mixture (see Figure 1C), led to rapid formation of PEGDA polymer (i.e., in situ polymerization or gelation), leading to remote capturing of cells and microparticles via a thread-like polymeric structures.

Polymerization of PEGDA monomers initiated inside the TRAP bot's reaction chamber. We incorporated a colored dye—Rhodamine (R6G, pink),[25,24] which upon polymerization, gets entrapped inside the hydrogel network and promoted easy visualization as depicted in **Figure 2**A. Highlighted region (marked via an arrow), shows lateral and transverse section of TRAP bots stained with R6G (pink), owing to the accumulation of R6G-polymerized hydrogel matrix inside the reaction microchamber. (See Figure S1 in the Supporting Information depicting SEM image of a TRAP bot with polymerized PEGDA at the reaction microchamber.)

Figure 2B shows TRAP bot with an elongated thread-like PEGDA polymer (over 500 µm, ≈two-body lengths) emerging from the reaction microchamber. The "polymeric tail" originated from the TRAP bot's reaction chamber and adhered onto the chassis (refer to Figure S2 in the Supporting Information depicting optical and SEM images of the corresponding TRAP bot). Interestingly, extruded PEGDA polymeric structures (Figure 2C), exhibited torsion along its axial plane (highlighted by a "white arrow"), resulting in a distinct coil-like polymeric assembly which is indicative of rapid polymerization during the step-growth phase (propagation).[26,27] This was further confirmed by an SEM imaging (Figure 2E) of the resulting polymeric thread-like structure, with ≈70 µm in length. Owing to the presence of coiling effect, tapered ends were ≈7 µm, with wide region ≈12 µm. Resulting polymeric thread-like microstructure had a porous network, as expected in case of a hydrogel, with mesh size of 400–600 nm as shown in Figure 2D. Such a porous network facilitates exchange of ions and nutrients for several chemical and biological applications.

Figure 3A shows PEGDA hydrogel formation via a turbidity measurement assay. Upon gelation (i.e., polymerization), PEGDA hydrogel shows increase in turbidity, which can intrinsically integrate the signal (absorbance@600 nm) from the full volume of hydrogel.[28] We utilized 1/10th of the initial concentration to enable time-dependent study of PEGDA polymerization—with (w/) and without (w/o) micromotors. As highlighted in Figure 3A, polymerization (gelation) in the presence of micromotors, i.e., Pt-catalyst (blue line) was completed in ≈8 min (i.e., 480 s), and the absorbance remained constant until the end of the reaction (10 min). On the contrary, PEGDA polymerization without micromotors, i.e., absence of Pt catalyst (red line), failed to achieve the chain-growth propagation

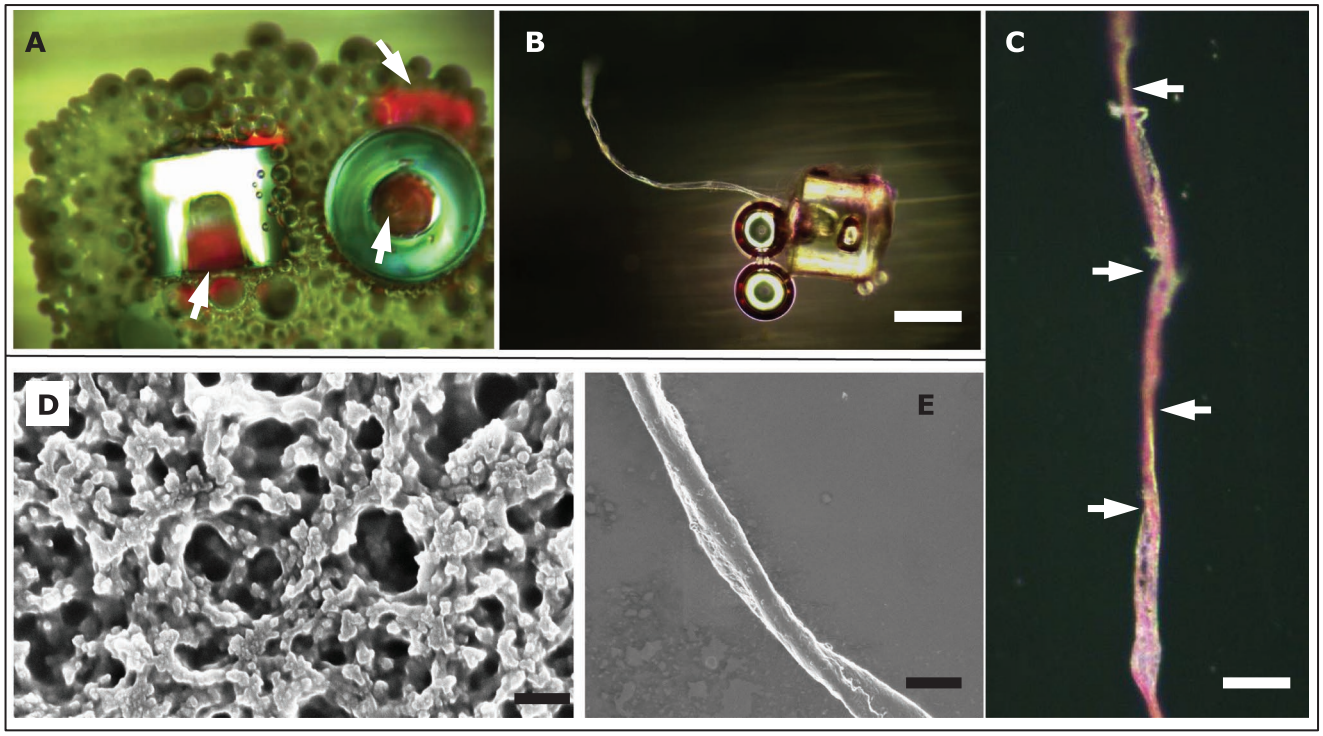

Figure 2. Optical imaging of TRAP bots depicting: A) polymer initiation inside the micromotor, B) activated TRAP bot with a distinct hydrogel "tail" (scale bar: 200 µm), and C) polymerized PEGDA thread-like microstructure (scale bar: 10 µm). D,E) SEM images highlighting: D) hydrogel porosity (scale bar: 500 nm) and E) microcoiling along the polymer structure (scale bar: 10 µm).

toward complete hydrogel formation. This also confirms the synergistic effect of the H_2O_2–Pt system toward free radical ($HO^{\bullet}$) generation for PEGDA polymerization.[29]

Polymerized acrylate hydrogel was confirmed by an FT-IR study (Figure 3B), which showed absence of $=CH_2$=CH– bonds at 1407 and 809 cm^{-1}, highlighting consumption of free acrylate group in the polymerized thread-like structures.[30] Also, decrease in relative peak intensity of carbonyl group (C=O) at 1720 cm^{-1} (monomer), and associated peak shifting from 1720 to 1728 cm^{-1}, confirmed acrylate polymerization.[31] Figure 3C shows TRAP bot reaction mechanism involving PEGDA polymerization and associated self-propulsion. Here, two independent free-radical reactions are synergistically acting together: 1) $FeCl_3$ (III) & ascorbic acid and 2) catalytic decomposition of H_2O_2 via Pt catalyst (acid). Rapid influx of free radicals in immediate acidic microenvironment, attacks the acrylate-end group of the monomers, resulting in polymer initiation and chain-propagation. Simultaneously, catalytic dissociation of H_2O_2 via a Pt catalyst also resulted in autonomous propulsion via an oxygen evolution reaction.[32] This should not be confused by a vanguard study by Pavlick et al. demonstrating an immobilized Grubb's catalyst onto a Janus NP (400 nm), such that upon enzymatic reaction with its substrate (norborene mixed in trichloroethane), a diffusophoretic displacement was observed.[33]

Figure 4A shows PEGDA polymerization and associated burst release of the resulting hydrogel from a TRAP bot. The entire reaction takes about 2 s, with ≈0.60 s for the polymeric-thread

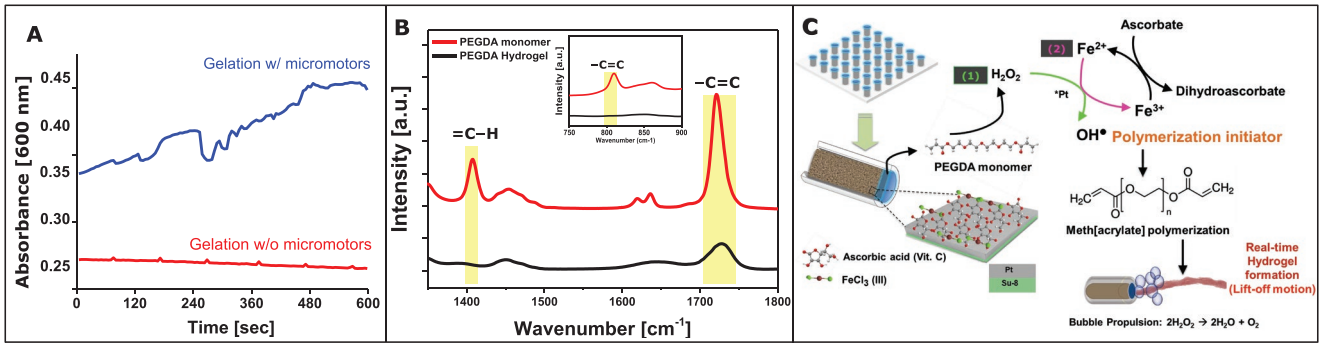

Figure 3. A) Effect of TRAP bots on PEGDA polymerization (turbidity measurement @600 nm), B) FT-IR spectra of the resulting PEGDA polymer (compared with the PEGDA monomer). C) Reaction mechanism of TRAP bot activation toward in situ gelation (thread-like microfibers) and autonomous propulsion.

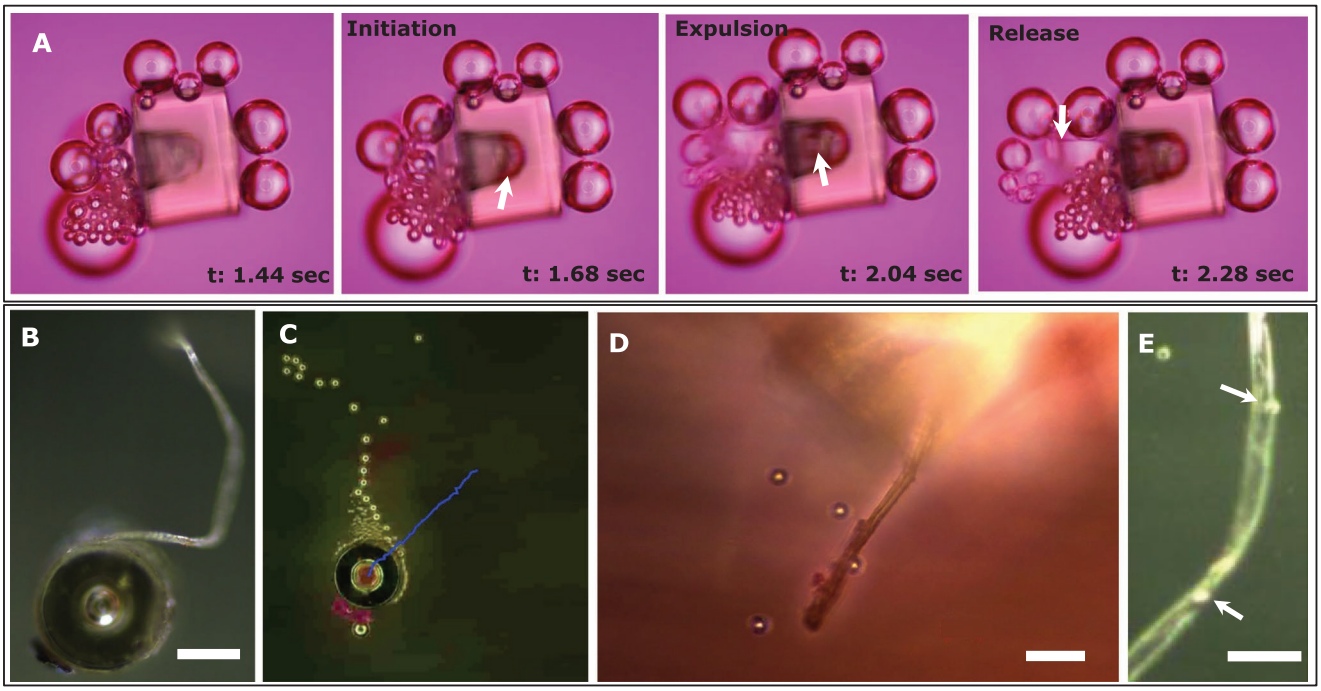

Figure 4. Optical images of TRAP bot activity: A) Real-time polymer formation and extrusion, B) TRAP bot with a distinct hydrogel tail (scale bar: 150 μm), C) Motion tracking profile of TRAP bot with attached PEGDA gel interface (H_2O_2: 5%), and D,E) trapping of polystyrene microparticles (10 μm) with the polymeric tail of TRAP bots (scale bar: 50 μm).

initiation and release. A three-step polymerization process was observed: i) polymerization initiation via mixing of radical and monomer inside the TRAP bot, ii) simultaneous expulsion of the polymer chain out of the microchamber via a bubble thrust mechanism, and iii) chain extension/termination, which controls the length of the polymeric tail, and is dependent on the reaction microenvironment. Please refer to Video S1 in the Supporting Information demonstrating real-time TRAP bot polymer synthesis. Figure 4B shows one such polymerized PEGDA hydrogel tail of size ≈400 μm, almost twice the size of the TRAP bot, protruding from the reaction microchamber. Owing to the presence of hydrogen peroxide, the observed TRAP bot depicted bubble propulsion (Figure 4C) with a swimming speed ≈90 ± 65 μm s^{-1} (n = 5). It is important to note that speed of such a micromotor, assuming constant substrate concentration (H_2O_2), will depends on active surface area of the catalyst, i.e., Pt layer in contact with the substrate. Here, each TRAP bot exhibits hydrogel formation inside the reaction chamber, which then covers the underlying Pt layer (depending upon site and degree of hydrogel formation), thereby "controlling" the total surface area in contact with the substrate. Clearly, there will be variable speeds with such a system, as also observed in our case. Also, refer to Video S2 in the Supporting Information. We anticipate that upon hydrogel initiation (i.e., PEGDA polymerization), there is an immediate increase in viscous forces,[34] which may impede the TRAP bot motion.[35,36] Protruding PEDGA polymeric-tail was able to entrap polystyrene (PS) microparticles (10 μm) as shown in Figure 4D,E. Upon polymer chain expulsion, a vertical liftoff motion is observed, which is further supported via a bubble propulsion. Note that in the absence of this vertical liftoff, no motion via a bubble propulsion is observed. Refer to Video S3 in the Supporting Information demonstrating real-time polymerization and assisted bubble propulsion via TRAP bots.

However, from biomedical perspective, "cellular engineering and biosensing applications would benefit from surfaces that allow robust anchoring of hydrogels and immobilization of proteins"—bubble propulsion is not a critical factor in this regard.[37,38] To this end, we also investigated cellular enmeshing and biocompatibility of TRAP bots in the absence of hydrogen peroxide, as shown in **Figure 5**. Note that the resulting TRAP bot assembly can still be magnetically guided/separated owing the presence of a Ni layer.

Real-time hydrogel formation and associated cell trapping was demonstrated in cell culture media as shown in Figure 5A (see Video S4 in the Supporting Information). Optical image shows a membrane intact fibroblast cell (indicated by a red arrow) attached on to the hydrogel-tail. Fibroblast cells were also enmeshed in the hydrogel network as shown in Figure 5B. To confirm that the polymerization process and associated polymerized hydrogel structure is nontoxic for living cells, a LIVE/DEAD assay was carried out upon cells entrapment, as shown in Figure 5C. The cell-permeant calcein AM dye was employed to label all viable cells with green fluorescence, while the red fluorescence of the membrane-impermeant dye ethidium homodimer (Eth-D1) can only be observed in dead cells with a ruptured cell membrane. Figure 5C shows viable fibroblast cells adhered onto the thread-like polymer structure upon radical polymerization, displaying green fluorescence only, confirming that there are no cytotoxic effects of polymerization on the trapped cells. Figure 5D shows a SEM image of NIH 3T3 fibroblast cells adhered onto the hydrogel interface

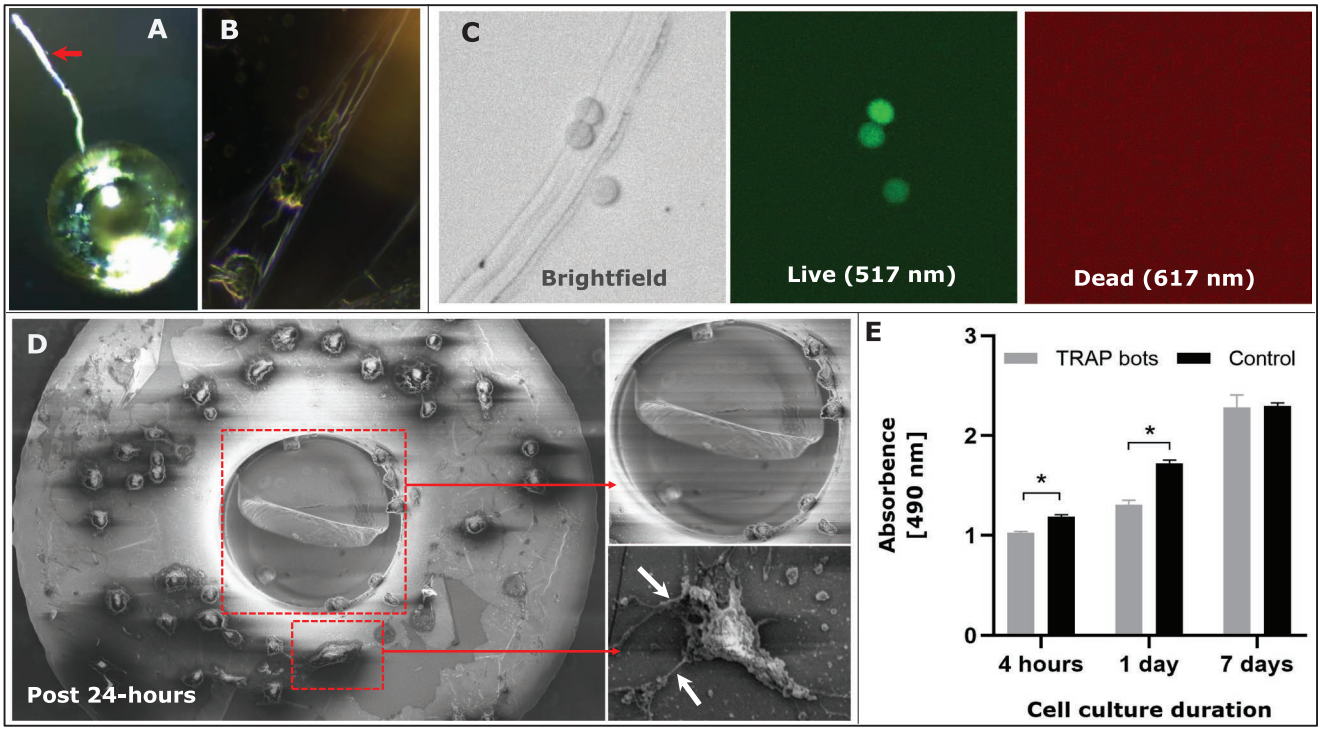

Figure 5. Cell study of TRAP bots depicting: A,B) Optical images showing cellular enmeshing of fibroblast cells. C) LIVE/DEAD assay of cells entrapped with the hydrogel thread-like structure. D) SEM image depicting cellular adhesion on a TRAP bot (Inset: (top) reaction microchamber; and (bottom) hydrogel laden TRAP bot's surface). E) MTS assay of TRAP bots (gray) compared to control (black) confirming their innate biocompatibility.

present over the TRAP bot surface. Figure 5D (inset, top) shows TRAP bot's reaction microchamber, with a clearly visible protruded hydrogel structure, and membrane intact fibroblast cells inside the reaction microchamber. Also, anchored cells demonstrated highly favorable response to the TRAP bots assembly post-polymerization (Figure 5D inset, bottom), with distinct cell anchorage on to the TRAP bot surface via focal adhesions (depicted with "white arrow"). Such focal adhesions are a common feature for spread cells on planar substrates depicting healthy mesenchymal migration.[39] Contrary to the common notion of cellular toxicity associated with metals like Ni/Pt, or traces of reaction mixture in the core, TRAP bots were found to be highly biocompatible as shown in Figure 5E. We performed an exhaustive 7 day study examining the metabolic activity of the NIH 3T3 fibroblast cells in the presence of TRAP bots via an MTS cell proliferation assay. The NAD(P)H-dependent dehydrogenase enzyme in metabolically active cells causes the reduction of MTS tetrazolium compound, generating a colored formazan product that is soluble in cell culture media, and can be quantified by measuring the absorbance at 490–500 nm. Initially, TRAP bots and their associated chemical reactions led to a lower metabolic activity of cells at both time points at 4 h (13.3% lower than control), and 24 h (23.9% lower than control). However, the cells adjusted well to the substrate and its microenvironment with no significant difference after 7 days. Clearly, there is an overall increase in growth trend with respect to culture time confirming the long-term biocompatibility of TRAP bots. Finally, owing to the presence of a Ni layer (10 nm), biocompatible TRAP bots are capable of magnetic guidance and separation (see Video S5 in the Supporting Information).

TRAP bots technology has several advantages as compared to prefabricated polymers including: i) prefabricated polymers are usually limited to seeding cells on the surface, leading to a 2D-like cell culture, but not cell enmeshing;[40–42] ii) comprehensive studies on physical behavior of single cells and also cell–matrix interactions,[43,44] and iii) an effective alternative to otherwise complex microsystems, which are designed and developed for single cell trapping and relevant studies.[44] For example, Fu et al.[45] developed a microfluidic system with an array of U-shaped PEGDA hydrogel microstructures. Cell entrapment was demonstrated by combining fluid flow, force of gravity, and the geometry of the microstructures.

In conclusion, independent developments in the area of hydrogel research and micromotors technology have opened a wide range of applications in several key-enabling technologies. This includes embedded microfluidics[46] versus micromotors-on-chip[47,48] and drug delivery via hydrogels[49] versus drug delivery via micromotors.[50] To the best of our knowledge, this is the first study reporting real-time, in situ hydrogel synthesis via a micromotor system. We envision that TRAP bots will set a new paradigm toward remote enmeshing of a "target" toward on-demand soft-theranostics, including site-directed cell/tissue grafting for bionic microsystems,[51] and novel nano/microencapsulation technologies. A recent study by Nitta et al. demonstrated a nanofiber diacrylate based hydrogel for metal adsorption from aqueous solution.[52] To this end, TRAP bots with their nanoporous interface will unravel novel applications in wastewater remediation via an on board, in situ gelation technology. One immediate area of exploration will be development of

suspension culture, of otherwise anchorage-dependent cell lines. Resulting suspension culture can be magnetically-controlled to induce desired flow gradients with easy harvesting, enabling production of commercially-important proteins/bioproducts,[53] including disease biomarkers,[54] as well as flow-dependent cell proliferation.[55] In future, development of biocompatible propulsion schemes, by incorporating immobilized enzymes and photopolymerization methods will be of significant interest for next-generation TRAP bots for biomedical applications,[56,57] i.e., remote assembly and guided differentiation of living cells via an artificial microbot.

Supporting Information

Supporting Information is available from the Wiley Online Library or from the author.

Acknowledgements

All authors acknowledge the assistance of Khorshid Kamguyan for PDMS negative mask and Lasse Thamdrup for cleanroom fabrication. S.K.S would like to thank H.C. Ørsted COFUND for funding. This project has received funding from the European Union's Horizon 2020 research and innovation programme under the Marie Skłodowska-Curie Grant Agreement No. 713683. All authors would like to acknowledge the Danish National Research Foundation (DNRF122) and Villum Fonden (Grant No. 9301) for Intelligent Drug Delivery and Sensing Using Microcontainers and Nanomechanics (IDUN).

Conflict of Interest

The authors declare no conflict of interest.

Keywords

biocompatible micromotors, in situ polymerization, live cell trapping, PEGDA hydrogel, remote tissue culture

Received: March 11, 2019
Revised: May 9, 2019
Published online:

[1] S. K. Srivastava, G. Clergeaud, T. L. Andresen, A. Boisen, *Adv. Drug Delivery Rev.* **2019**, *138*, 41.
[2] S. Sanchez, A. A. Solovev, S. Schulze, O. G. Schmidt, *Chem. Commun.* **2011**, *47*, 698.
[3] Y. Alapan, O. Yasa, O. Schauer, J. Giltinan, A. F. Tabak, V. Sourjik, M. Sitti, *Sci. Rob.* **2018**, *3*, eaar4423.
[4] B. E. F. De Ávila, P. Angsantikul, J. Li, M. Angel Lopez-Ramirez, D. E. Ramírez-Herrera, S. Thamphiwatana, C. Chen, J. Delezuk, R. Samakapiruk, V. Ramez, M. Obonyo, L. Zhang, J. Wang, *Nat. Commun.* **2017**, *8*, 272.
[5] S. K. Srivastava, O. G. Schmidt, *Chem.-Eur. J.* **2016**, *22*, 9072.
[6] S. K. Srivastava, M. Medina-Sanchez, O. G. Schmidt, *Chem. Commun.* **2017**, *53*, 8140.
[7] V. M. Fomin, M. Hippler, V. Magdanz, L. Soler, S. Sanchez, O. G. Schmidt, *IEEE Trans. Rob.* **2014**, *30*, 40.
[8] W. F. Paxton, S. Sundararajan, T. E. Mallouk, A Sen, *Angew. Chem., Int. Ed.* **2006**, *45*, 5420.
[9] T. Patiño, N. Feiner-Gracia, X. Arqué, A. Miguel-López, A. Jannasch, T. Stumpp, E. Schäffer, L. Albertazzi, S. Sánchez, *J. Am. Chem. Soc.* **2018**, *140*, 7896.
[10] J. Li, X. Yu, M. Xu, W. Liu, E. Sandraz, H. Lan, J. Wang, S. M. Cohen, *J. Am. Chem. Soc.* **2017**, *139*, 611.
[11] S. K. Srivastava, M. Guix, O. G. Schmidt, *Nano Lett.* **2016**, *16*, 817.
[12] A. Kaiser, H. H. Wensink, H. Löwen, *Phys. Rev. Lett.* **2012**, *108*, 268307.
[13] L. Restrepo-Pérez, L. Soler, C. S. Martínez-Cisneros, S. Sánchez, O. G. Schmidt, *Lab Chip* **2014**, *14*, 1515.
[14] S. E. Hulme, W. R. DiLuzio, S. S. Shevkoplyas, L. Turner, M. Mayer, H. C. Berg, G. M. Whitesides, *Lab Chip* **2008**, *8*, 1888.
[15] M. G. L. Van Den Heuvel, C. T. Butcher, R. M. M. Smeets, S. Diez, C. Dekker, *Nano Lett.* **2005**, *5*, 1117.
[16] D. A. Wilson, R. J. M. Nolte, J. C. M. Van Hest, *J. Am. Chem. Soc.* **2012**, *134*, 9894.
[17] M. W. Tibbitt, K. S. Anseth, *Biotechnol. Bioeng.* **2009**, *103*, 655.
[18] I. Tokarev, S. Minko, *Adv. Mater.* **2010**, *22*, 3446.
[19] G. Jeon, S. Y. Yang, J. Byun, J. K. Kim, *Nano Lett.* **2011**, *11*, 1284.
[20] S. Ma, M. Scaraggi, D. Wang, X. Wang, Y. Liang, W. Liu, D. Dini, F. Zhou, *Adv. Funct. Mater.* **2015**, *25*, 7366.
[21] K. Uh, B. Yoon, C. W. Lee, J. M. Kim, *ACS Appl. Mater. Interfaces* **2016**, *8*, 1289.
[22] G. Orive, E. Santos, D. Poncelet, R. M. Hernández, J. L. Pedraz, L. U. Wahlberg, P. De Vos, D. Emerich, *Trends Pharmacol. Sci.* **2015**, *36*, 537.
[23] L. Sun, S. Zhang, J. Zhang, N. Wang, W. Liu, W. Wang, *J. Mater. Chem. B* **2013**, *1*, 3932.
[24] L. M. Johnson, C. A. DeForest, A. Pendurti, K. S. Anseth, C. N. Bowman, *ACS Appl. Mater. Interfaces* **2010**, *2*, 1963.
[25] Y. Wu, S. Joseph, N. R. Aluru, *J. Phys. Chem. B* **2009**, *113*, 3512.
[26] B. V. Shankar, A. Patnaik, *J. Phys. Chem. B* **2007**, *111*, 9294.
[27] K. J. Nagy, M. C. Giano, A. Jin, D. J. Pochan, J. P. Schneider, *J. Am. Chem. Soc.* **2011**, *133*, 14975.
[28] K. H. Malinowska, T. Verdorfer, A. Meinhold, L. F. Milles, V. Funk, H. E. Gaub, M. A. Nash, *ChemSusChem* **2014**, *7*, 2825.
[29] A. D. Bokare, W. Choi, *J. Hazard. Mater.* **2014**, *275*, 121.
[30] A. F. Visentin, T. Dong, J. Poli, M. J. Rapid Panzer, *J. Mater. Chem. A* **2014**, *2*, 7723.
[31] S. Bäckström, J. Benavente, R. W. Berg, K. Stibius, M. Larsen, H. Bohr, C. Hélix-Nielsen, *Mater. Sci. Appl.* **2012**, *3*, 425.
[32] D. Yamamoto, A. Shioi, *KONA Powder Part. J.* **2015**, *32*, 2.
[33] R. A. Pavlick, S. Sengupta, T. McFadden, H. Zhang, A Sen, *Angew. Chem., Int. Ed.* **2011**, *50*, 9374.
[34] Y. D. Park, N. Tirelli, J. A. Hubbell, *The Biomaterials: Silver Jubilee Compendium*, Elsevier Science, The Netherlands **2006**, pp. 203–210.
[35] L. Zhu, E. Lauga, L. Brandt, *Phys. Fluids* **2012**, *24*, 051902.
[36] J. R. Gomez-Solano, A. Blokhuis, C. Bechinger, *Phys. Rev. Lett.* **2016**, *116*, 138301.
[37] J. H. Seo, D. S. Shin, P. Mukundan, A. Revzin, *Colloids Surf., B* **2012**, *98*, 1.
[38] S. K. Srivastava, V. G. Yadav, *Trends Biotechnol.* **2018**, 483.
[39] B. Koch, A. K. Meyer, L. Helbig, S. M. Harazim, A. Storch, S. Sanchez, O. G. Schmidt, *Nano Lett.* **2015**, *15*, 5530.
[40] S. R. Caliari, J. A. Burdick, *Nat. Methods* **2016**, *13*, 405.
[41] B. M. Baker, C. S. Chen, *J. Cell Sci.* **2012**, *125*, 3015.
[42] G. D. Nicodemus, S. J. Bryant, *Tissue Eng., Part B* **2008**, *14*, 149.
[43] X. Gong, K. L. Mills, *Sci. Rep.* **2018**, *8*, 3849.
[44] T. Braschler, R. Johann, M. Heule, L. Metref, P. Renaud, *Lab Chip* **2005**, *5*, 553.
[45] C.-Y. Fu, S.-Y. Tseng, S.-M. Yang, L. Hsu, C.-H. Liu, H.-Y. Chang, *Biofabrication* **2014**, *6*, 015009.

[46] S. Allazetta, T. C. Hausherr, M. P. Lutolf, *Biomacromolecules* **2013**, *14*, 1122.
[47] L. Baraban, D. Makarov, R. Streubel, I. Mönch, D. Grimm, S. Sanchez, O. G. Schmidt, *ACS Nano* **2012**, *6*, 3383.
[48] L. Restrepo-Pérez, L. Soler, C. Martínez-Cisneros, S. Sánchez, O. G. Schmidt, *Lab Chip* **2014**, *14*, 2914.
[49] A. Vashist, A. Vashist, Y. K. Gupta, S. Ahmad, *J. Mater. Chem. B* **2014**, *2*, 147.
[50] S. K. Srivastava, M. Medina-Sánchez, B. Koch, O. G. Schmidt *Adv. Mater.* **2016**, *28*, 832.
[51] S. K. Srivastava, V. G. Yadav, *Trends Biotechnol.* **2018**, *36*, 483.
[52] S. Nitta, M. Akagi, H. Iwamoto, *Polym. J.* **2019**, *51*, 501.
[53] O. W. Merten, *Philos. Trans. R. Soc., B* **2015**, *370*, 20140040.
[54] C. E. Yoo, J.-M. Park, H.-S. Moon, J.-G. Joung, D.-S. Son, H.-J. Jeon, Y. J. Kim, K.-Y. Han, J.-M. Sun, K. Park, D. Park, W.-Y. Park, *Sci. Rep.* **2016**, *6*, 37392.
[55] H. J. Kim, D. E Ingber, *Integr. Biol.* **2013**, *5*, 1130.
[56] T. Billiet, M. Vandenhaute, J. Schelfhout, S. Van Vlierberghe, P. Dubruel, *Biomaterials* **2012**, *33*, 6020.
[57] M. Guvendiren, J. A Burdick, *Curr. Opin. Biotechnol.* **2013**, *24*, 841.